THE SEAMOUNT AS A NOISE BARRIER

by

Herman Medwin, Emily Childs* and Edgar A. Jordan**
Physics Department, Naval Postgraduate School, Monterey, CA 93940, U.S.A.

ABSTRACT

When the path from a localized noise source is intercepted by a seamount the shielded noise consists of a diffracted component and, if the seamount is close to a sufficiently smooth ocean surface, a multiply-reflected component as well. The magnitude and frequency filtering of the blockage caused by the seamount is here determined by using the impulse solution of diffraction by a rigid wedge as a module for the computer calculation of multiple diffraction at gross changes of slope along the seamount and at its crest line. These computer calculations are validated by comparison with laboratory measurements using a scale model of DICKENS Seamount which has previously been shown to be an effective technique for the calculation of topographical diffraction at sea.

BACKGROUND

The ambient noise measured at any location depends on the noise source and the transmission path. A factor that may significantly affect the propagation loss is the interception of the noise path by a seamount; shadowing losses of 15 to 20 dB are commonly measured.

One successful technique for the prediction of shadowing losses by a seamount is the use of a 2M x 2M laboratory scale model[1] (Figs. 1,2); the scaled frequency-dependent diffraction losses at the seamount are added to the losses in the body of the sea which are calculated by a computer model such as FACT. There is good agreement with ocean data (Figs. 3,4). The seamount is assumed to be rigid; no other assumptions are needed. The increase of shadowing loss with frequency$^{1/2}$ has since been observed in several ocean experiments by different laboratories[2]. Whether this diffraction component is dominant depends on the distance between the seamount and the sea surface as well as the roughness of the sea surface[3].

*Ocean Acoustics Associates
**LT, U.S. Navy

In the example studied, DICKENS Seamount with a slope of about 14° culminating in a crest approximately 500M from the surface, a 35 knot wind resulted in an ocean surface of rms height 1.6M calculated from the Pierson-Moskowitz wind wave spectrum. In this case, the model studies show that not only was the diffraction component the first, it was also the largest component; multiple reflections between the seamount and the wind blown sea produced a much weaker signal. Note signal after 203 μs in Fig. 5

The physical basis for the interpretation of the diffraction is the fact that the diffracted energy comes principally from a region near the sound ray track. The crestline of the seamount at the sound track may be approximately most simply by the apex of a flat wedge; the rigorous closed form impulse solution of a rigid wedge is given by[4] eqs. (1)-(3),

$$p(t) = (-S\rho c/4\pi\theta_w)\{\beta\}[rr_0 \sinh y]^{-1} \exp(-\pi y/\theta_w), \tag{1}$$

where

$$\beta = \frac{\sin[(\pi/\theta_w)(\pi \pm \theta \pm \theta_0)]}{1 - 2\exp(-\pi y/\theta_w)\cos[(\pi/\theta_w)(\pi \pm \theta \pm \theta_0)] + \exp(-2\pi y/\theta_w)}, \tag{2}$$

$$y = \operatorname{arc\,cosh} \frac{c^2 t^2 - (r^2 + r_0^2 + Z^2)}{2rr_0} . \tag{3}$$

The term $(\pi \pm \theta \pm \theta_0)$ is written for simplicity; the curly bracket consists of the sum of four terms obtained by using the four possible combinations of the angles, $\pm\theta$ and $\pm\theta_0$.

Source coordinates are $(r_0, \theta_0, 0)$, receiver coordinates are (r, θ, Z). The angle of the wedge measured in the fluid region is called θ_w.

The sound diverges spherically from the point source and cylindrically from the crestal line scatterer. The earliest, strongest, pressure arrivals vary as $(\text{time})^{-1/2}$, and the frequency dependence of the scatter goes as $f^{1/2}$. For these reasons, the appropriate model scaling parameter is the far field diffraction strength, DS, given by

$$DS = 20 \log_{10} [(P_D/P_0)(r_0/R_0)(r/\lambda)^{1/2}] \tag{4}$$

where

P_D = diffracted pressure
P_0 = reference pressure at range R_0
R_0 = reference range (=1 M)
λ = wave length
r_0 = range, source to diffracting edge
r = range, diffracting edge to receiver

The far field diffraction strength is a function of wedge angle, angle of incidence, elevation and azimuthal scatter angles.

The concept of diffraction strength is used throughout this work. To convert to diffraction loss DL in dB one uses

$$DL = 20 \log_{10} [(r_o/R_D)(r/\lambda)^{1/2}] - DS \qquad (5)$$

where R_D is the direct range from source to receiver.

The equivalence of DS in the laboratory, where dimensions are measured in centimeters and frequencies go to 100kHz, and in the ocean with ranges in Km and frequencies in hundreds of Hertz, is shown in Fig. 6.

The asymptotic approach to the far field diffraction strength is presented as a function of r/λ in Fig. 7. It will be noted that the plane 14° wedge, the simplest approximation to the seamount, has a DS some 10dB too high; and the "contour wedge" which is contoured to the seamount profile along the sound track, and which is the physical realization of the two dimensional parabolic equation solution, is also several dB too high.

METHOD

The purpose of this paper is to demonstrate the extent to which the diffraction strength of the seamount may be determined by simple computer models based on plane wedge diffraction. The degree of validity of each computer model is measured by its ability to match the results of the laboratory scale model, whose effectiveness has already been proven by comparison with ocean experiments. Three types of computer models are considered: (1) a double wedge interpretation of the two-dimensional contour of a seamount; (2) a segmented plane wedge idealization of the crest of the three-dimensional seamount; (3) a multiple wedge reepresentation of the three-dimensional seamount.

Model 1:
Impulse calculations of double diffraction [6,7] have been used to describe the noise shadowing by a thick barrier. An example of the success of this technique for a thick plate is shown in Fig. 8. The two-dimensional double diffraction technique is now used to approximate the seamount as a wide barrier with two changes of slope; diffraction at the first edge is interpreted as due to a line of properly-timed secondary sources which reradiate over the second edge. Fig. 9 presents the two-dimensional Track 6 ray path contour of DICKENS seamount and two different approximations for the double diffraction calculations. In approximation one, plane surfaces are assumed from the source to position a where the sound diffracts through angle $\theta_W = 186°$, from a to position c where the diffraction angle is $\theta_W = 210°$, and from c to the receiver. In approximation two, the assumed plane surfaces are from source to b, b to d, and d to receiver; the two wedges thereby defined have $\theta_W = 212°$ and 186° at b and d, respectively. The comparison of the double diffraction computer calculation with laboratory experiment shows good to excellent agreement.

Model 2:
A naïve assumption will now be evaluated, namely that the crest of the three-dimensional seamount is where most of the major changes of slope occur, and that this may be approximated by crestal line segments of finite length, Fig. 10. Each segment produces a response that is a truncation[5] of the temporal response given by eq. (1), due to the limited time of interaction with the finite segment. The diffraction at the crest is then comprised of the sum of the plane wedge impulse responses. When this sum of the segmental responses for DICKENS Seamount is transformed to the frequency domain one obtains the DS shown in Fig. 10. Only the lowest frequencies are seen to be in agreement with experiment, as one should expect for this plane wedge model which ignores changes of slope along the slopes of the seamount. The DS of this crestal segment model is 1 or 2 dB better than that of the simple plane wedge, $\theta_w = 208°$, but it is still about 10 dB too large, compared with laboratory measurements.

Model 3:
The correct calculation should consider the multiple diffraction at all significant changes of slope at, and adjacent to, the ray path. The simplifying assumption is now made that we can visually identify the major changes of slope near TRACK 6 and use these for an adequate calculation of DS. Several wedge identifications have been made at regions of large change of slope. Fig. 11 shows these wedge approximations drawn on a photograph of the critical part of the seamount model. We find (Fig. 12) that computer calculations for four such approximations are within 2, 3 dB of each other and about 2 or 3 dB too high compared to the scale model experiment. The identification of larger numbers of changes of slope would be needed to improve the accuracy of the shadowing prediction.

CONCLUSIONS

Using topographical data that show the lines of significant changes of slope, the double diffraction technique permits accurate computer calculations of the diffraction loss of noise in the shadow of a two-dimensional seamount, and approximate predictions for the three-dimensional body.

ACKNOWLEDGEMENT

The comparison of our predictions with the results of ocean experiments was made possible by the generous cooperation of Gordon Ebbeson, N. Ross Chapman and the Defense Research Establishment Pacific, Victoria, B.C., Canada. This work was supported by the U.S. Office of Naval Research.

REFERENCES

1. H. Medwin and R.P. Spaulding, Jr., "The seamount as a diffracting body" in Bottom-Interacting Ocean Acoustics, W.A. Kuperman and F.B. Jensen eds., Plenum Press, New York, 1980.

2. H. Medwin, Chairman "Panel discussion of topographical effects on ocean propagation". J. Acoust. Soc. Am. 69, Suppl 1, S60 (Spring 1981).

3. E.A. Jordan and H. Medwin, "Scale model studies of scattering and diffraction at a seamount", J. Acoust. Soc. Am. 69, Suppl. 1, S59(1981).

4. M.A. Biot and I. Tolstoy, "Formulation of wave propagation in infinite media by normal coordinates with an application to diffraction", J. Acoust. Soc. Am. 29, 381-391 (1957). See also, I. Tolstoy, Wave Propagation (McGraw-Hill, New York, 1973).

5. H. Medwin, "Shadowing by finite barriers", J. Acoust. Soc., 9, 1060-1064 (1981).

6. H. Medwin, "Impulse studies of scattering by finite barriers", J. Acoust. Soc. Am. 71, Suppl. 1, S35(1982).

7. H. Medwin, E. Childs and G.M. Jebsen, "Impulse studies of double diffraction: a discrete Huygens interpretation", in press.

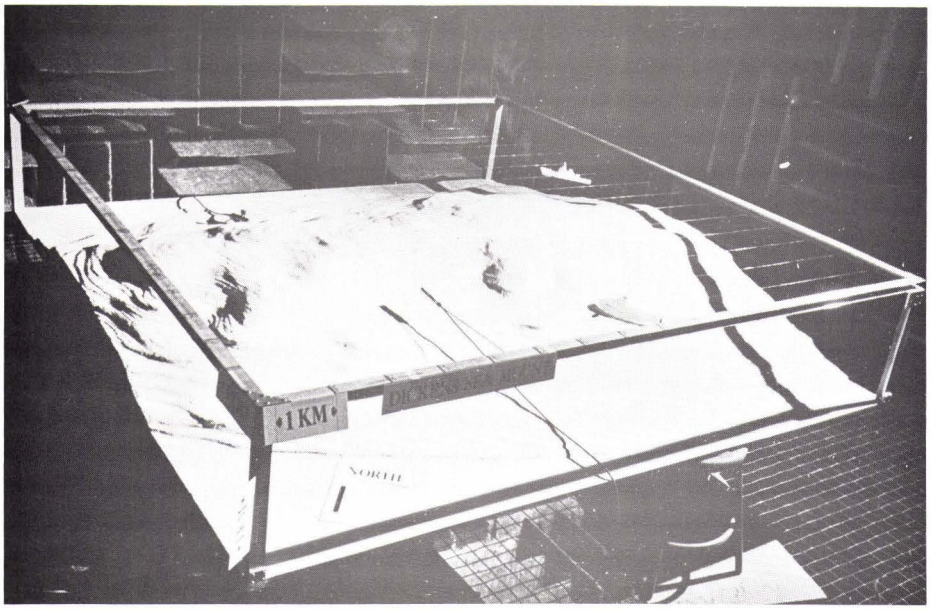

FIG. 1 LABORATORY MODEL OF DICKENS SEAMOUNT TO SCALE 1 km = 5 inches

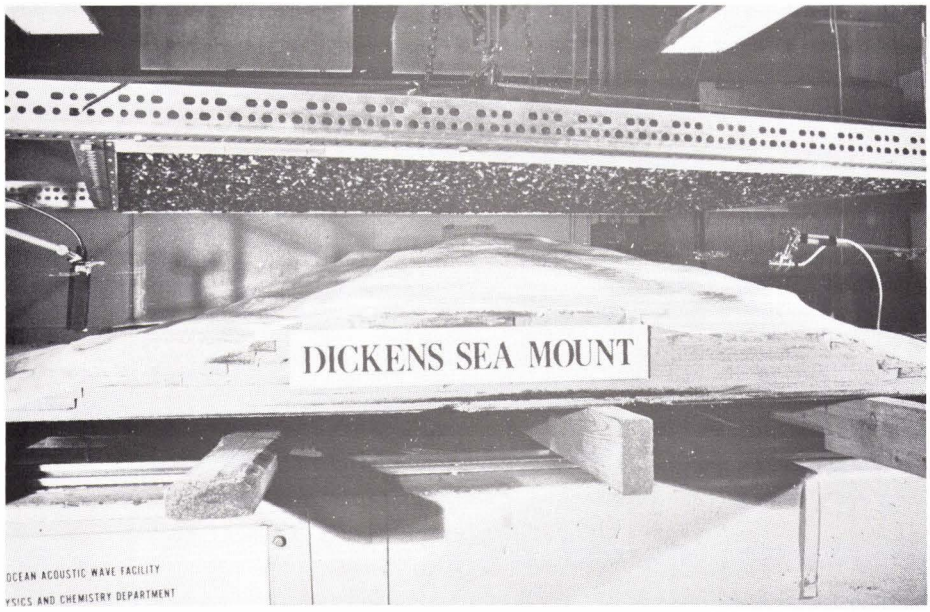

FIG. 2 LABORATORY MODEL OF DICKENS SEAMOUNT WITH SCALED MODEL OCEAN REPRESENTING 35 kn WIND CALCULATED FROM PIERSON-MOSKOWITZ WIND WAVE SPECTRUM

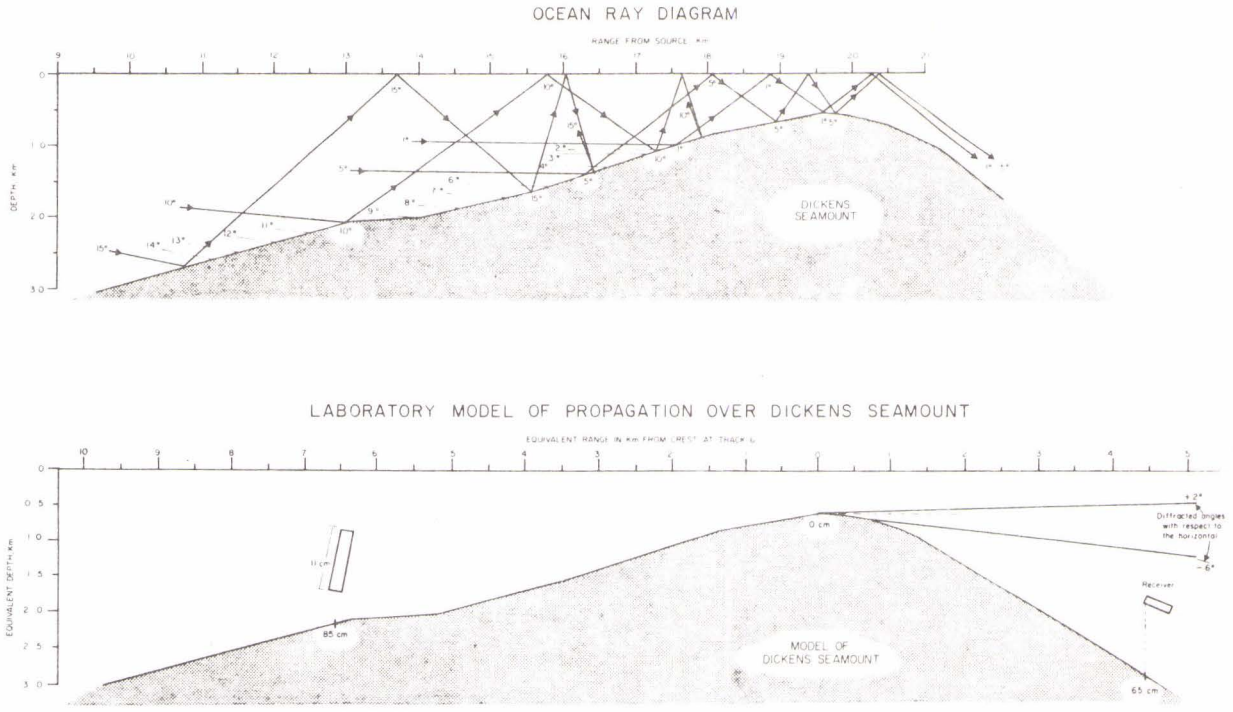

FIG. 3 RAY DIAGRAM OF FORWARD SCATTER AND DIFFRACTION BY DICKENS SEAMOUNT ALONG TRACK 6 OF THE OCEAN EXPERIMENT

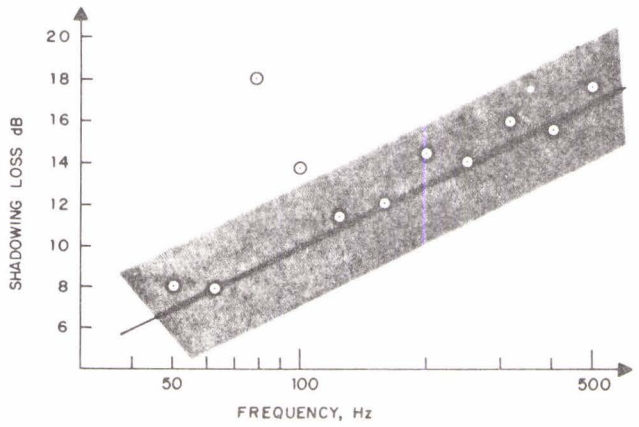

FIG. 4 PREDICTED SHADOWING LOSS CAUSED BY DICKENS SEAMOUNT FOR SOURCE-RECEIVER CASE SHOWN IN FIG. 3. Shaded area shows error bounds of scale model calculation. Circles are ocean data provided by N.R. Chapman and G.R. Ebbeson, Defense Research Establishment, Pacific, Victoria B.C., Canada. The theoretical slope, solid line, is 3 dB/octave

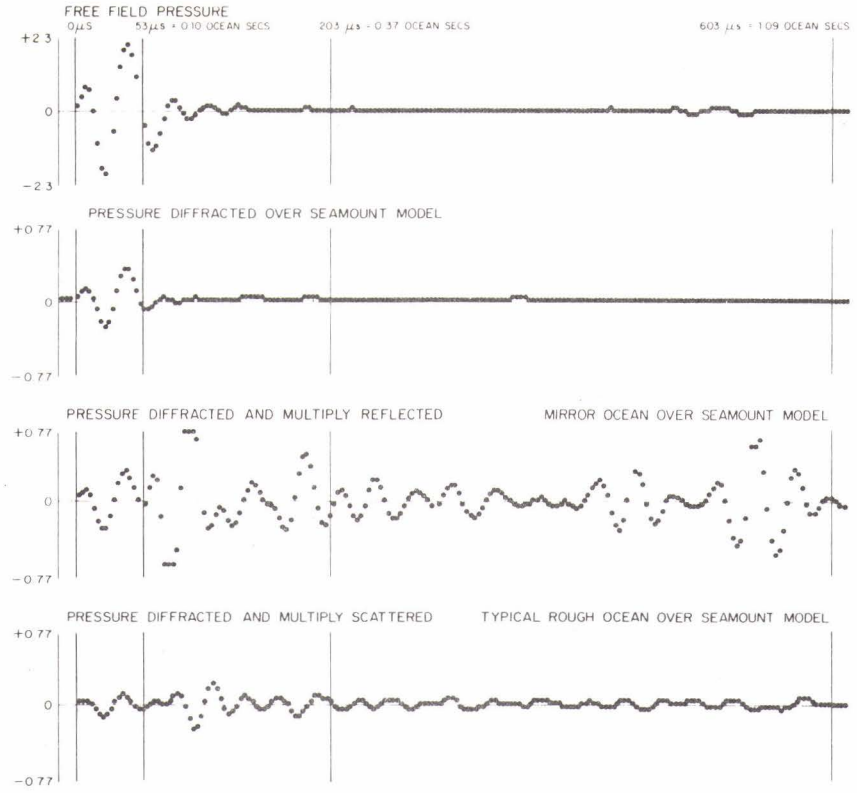

FIG. 5 LABORATORY STUDY OF IMPULSE DIFFRACTION AND MULTIPLE REFLECTION AT DICKENS SEAMOUNT. Top, free field pressure of source; second graph, pressure diffracted over seamount model; third graph, pressure diffracted and multiply reflected by a mirror smooth ocean surface; bottom graph, pressure diffracted and multiply reflected at a model sea surface for a 35 kn wind. The first 50 microseconds is the diffracted signal; from 50 to 203 μsec is scale model reflection scatter that does not occur at sea; from 203 μsec the signal is multiple scatter that represents the ocean situation

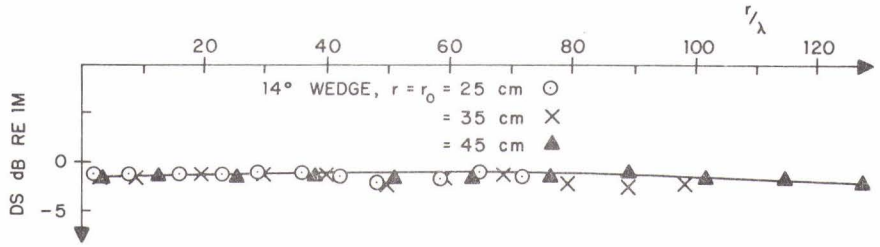

FIG. 6 DIFFRACTION STRENGTH, DS, FOR A SYMMETRICAL PLANE RIGID WEDGE WITH θ_w = 208° and Z = 0' The solid line gives the theoretical value for r = r_o = 3.5 km in water; data points are for a laboratory model experiment in air at three ranges, 25, 35 and 45 cm

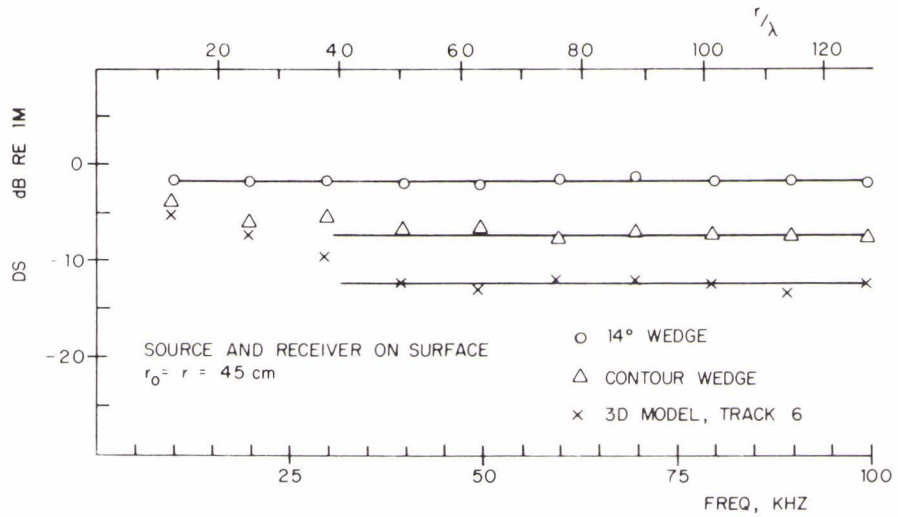

FIG. 7 DIFFRACTION STRENGTHS FOR THREE MODELS OF DICKENS SEAMOUNT. Solid lines from top to bottom are: theory for plane wedge of $\theta_w = 208°$*; asymptote for the two-dimensional contour wedge along the sound track; asymptote for the three-dimensional model along the sound track. Experimental data given by circles, triangles and crosses, respectively.*

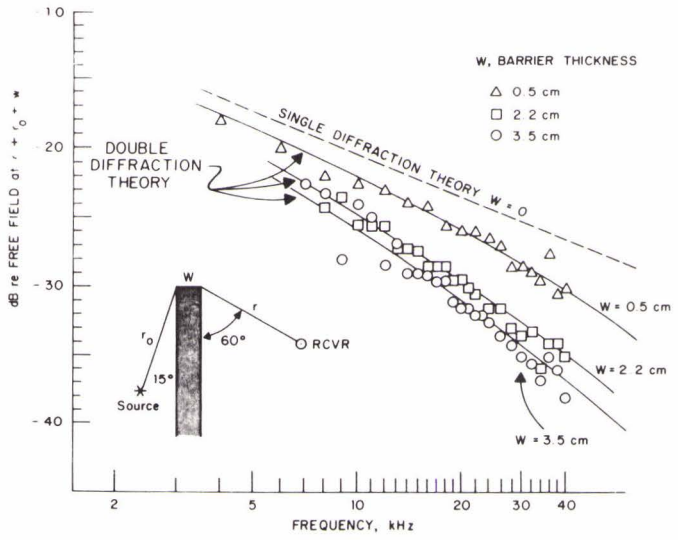

FIG. 8 SHADOWING LOSSES BY DOUBLE DIFFRACTION CALCULATIONS, SOLID LINES, COMPARED WITH EXPERIMENTAL MEASUREMENTS FOR THICK PLATES. The ranges are $r = r_o = 25$ *cm*

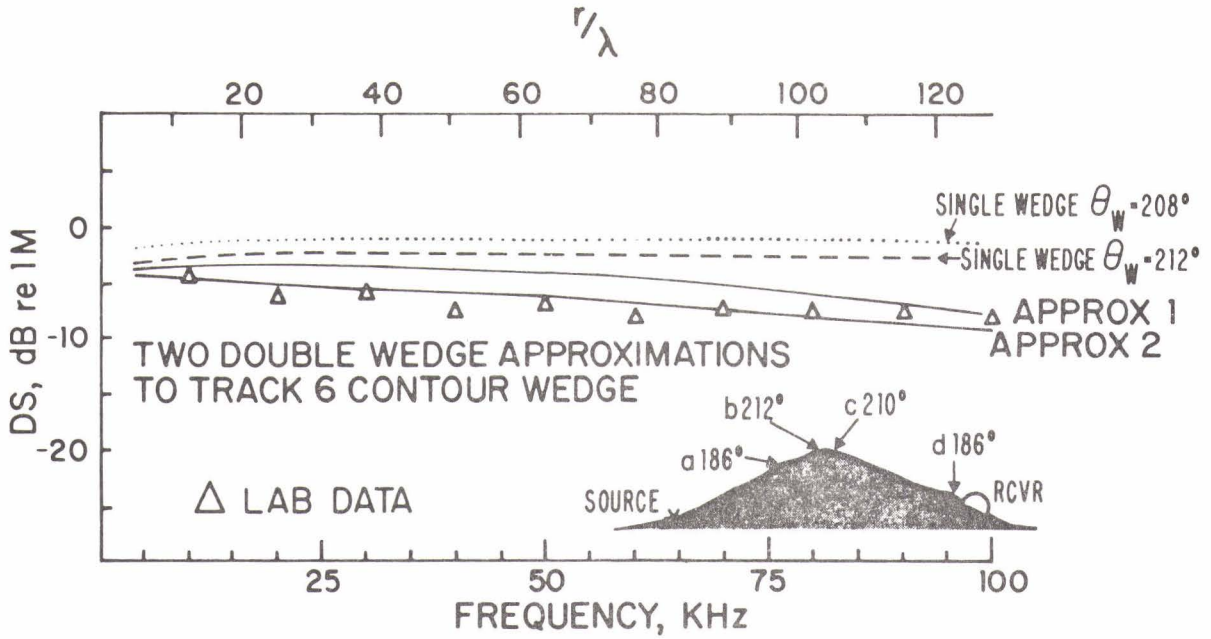

FIG. 9 TWO DOUBLE DIFFRACTION COMPUTER CALCULATIONS OF DIFFRACTION STRENGTH COMPARED WITH LABORATORY EXPERIMENTAL MEASUREMENTS OF THE TWO-DIMENSIONAL "CONTOUR MODEL" OF SOUND TRACK 6 OVER DICKENS SEAMOUNT. The double diffraction barriers are plane surface fittings to the true contour (inset). Single plane wedge theory for θ_w = 208° (14° slopes) and θ_{ww} = 212° (16° slopes) are shown for comparison

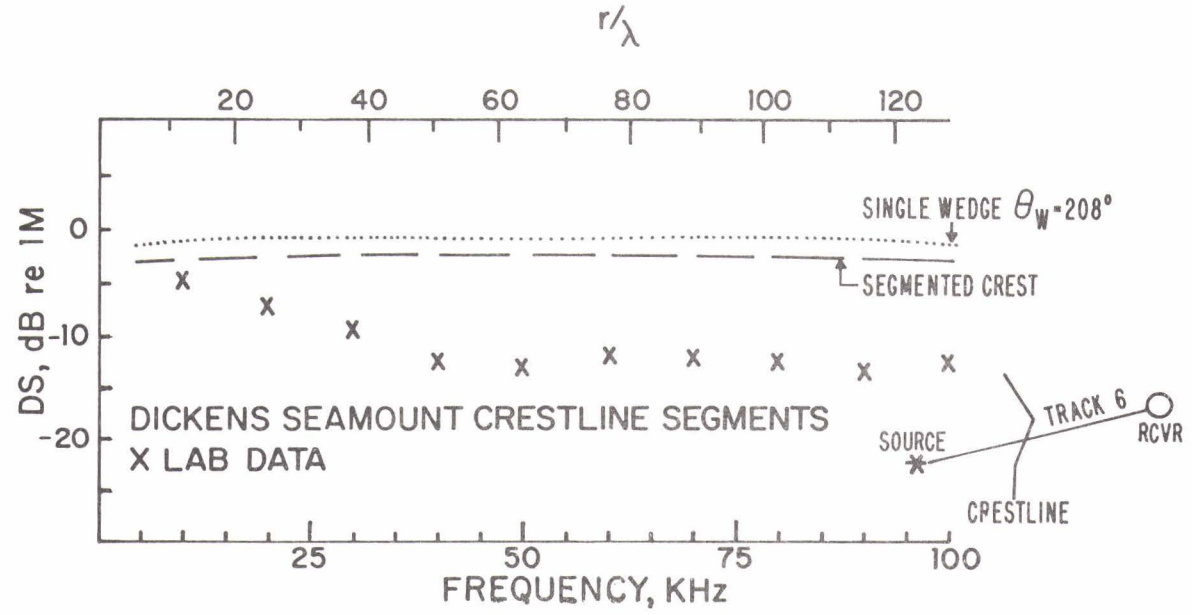

FIG. 10 PREDICTED DS FOR CRESTLINE SEGMENTAL WEDGES AS SHOWN IN INSET. Laboratory measurements for DS for scale model of DICKENS seamount shown by crosses. The dotted line is the solution for a single plane wedge θ_w = 208°.

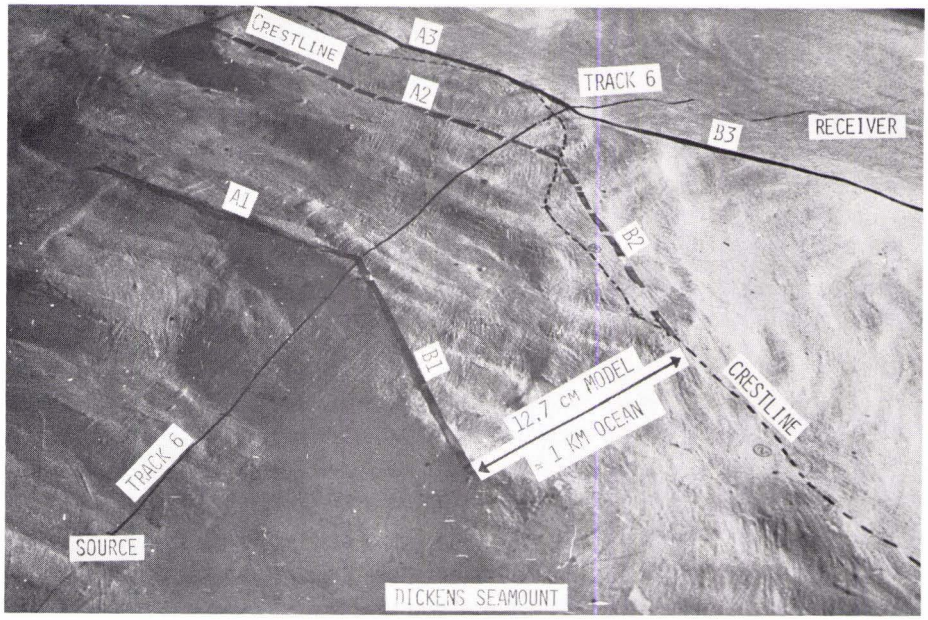

FIG. 11 PHOTOGRAPH OF THE DICKENS SEAMOUNT MODEL WITH IDENTIFICATION OF WEDGE CRESTS USED FOR THE DOUBLE DIFFRACTION CALCULATIONS NEAR SOUND TRACK 6

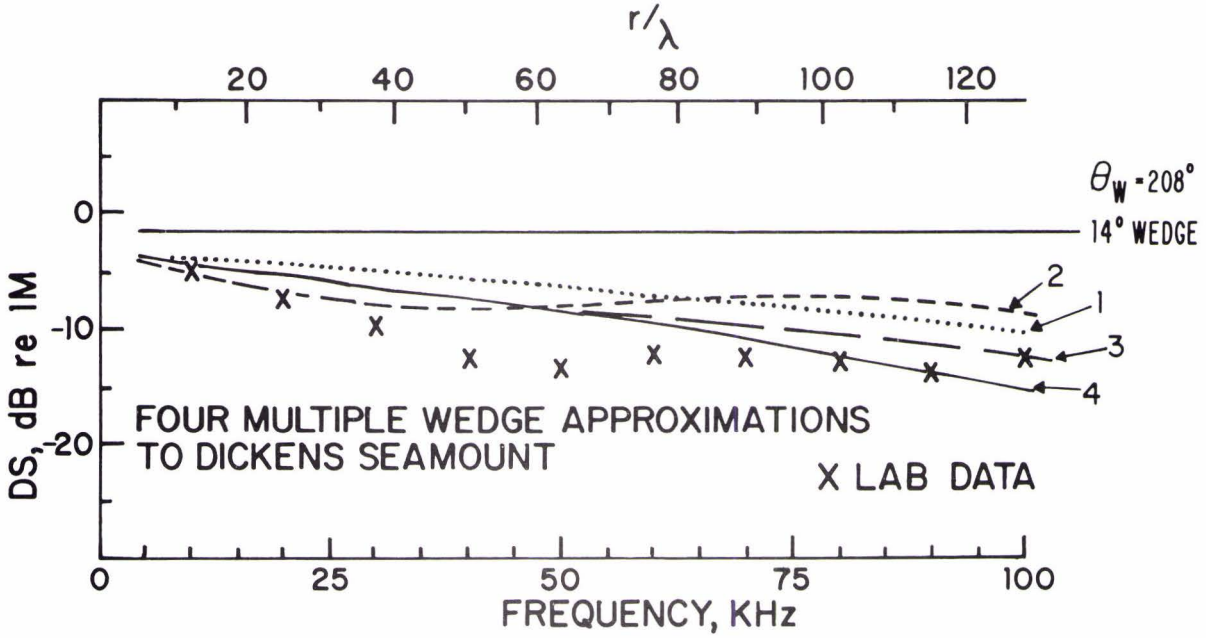

FIG. 12 MULTIPLE DIFFRACTION CALCULATIONS OF DS FOR WEDGES THAT ADJOIN THE PRINCIPAL RAY PATH CONTOUR (TRACK 6) COMPARED WITH LABORATORY MEASUREMENTS FROM THE THREE DIMENSIONAL SCALE MODEL OF DICKENS SEAMOUNT. Referring to Fig. 11, approximation 1 consists of segments A1 and B1 and a wedge between A2 and A3 and between B2 and B3. Approximation 2 is comprised of the double wedge A1, A2 and double wedge B1, B2. Approximation 3 uses a wedge between A2, A3 and B2, B3 and a second (unmarked) wedge closer to the receiver. Approximation 4 is a triple diffraction which is composed of wedges A1, B1 and A2, B2 and A3, B3